

Research article

Bone Tropism of Prostate Cancer Metastasis is Augmented by Activation of EphA2 Noncanonical Signaling and Ligand-Deficient Skeletal Microenvironment

Ryan Lingerak^{#1,3}, Aaron Petty^{#3}, Hong Guo³, Xiaojun Shi³, Soyeon Kim³, Hebei Lin⁴, Jer-Tsong Hsieh⁵, Dean G. Tang⁶, Bangyan Stiles⁷, David Wald⁸, Sooryanarayana Varambally⁹, Zhenghong Lee^{2,10}, Arul M. Chinnaiyan¹¹, Colm Morrissey¹², Bingcheng Wang^{*1,2,3}

1. Department of Physiology and Biophysics, Case Western Reserve University, Cleveland, OH, USA

2. Case Comprehensive Cancer Center, Cleveland, OH, USA

3. Division of Cancer Biology, MetroHealth Center for Cancer Research, MetroHealth Campus, Case Western Reserve University, Cleveland, OH, USA

4. Department of Biochemistry, Case Western Reserve University, Cleveland, OH, USA

5. Department of Urology, University of Texas Southwestern Medical Center, Dallas, TX, USA

6. Department of Pharmacology & Therapeutics, Roswell Park Comprehensive Cancer Center, Buffalo, NY, USA

7. Department of Pharmacology and Pharmaceutical Sciences, University of Southern California, Los Angeles, CA, USA

8. Department of Pathology, Case Western Reserve University, Cleveland, OH, USA

9. Department of Pathology, University of Alabama at Birmingham, Birmingham, AL, USA

10. Department of Radiology, Case Western Reserve University, Cleveland, OH, USA

11. Michigan Center for Translational Pathology, University of Michigan, Ann Arbor, MI, USA

12. Department of Urology, University of Washington, Seattle, WA, USA

These authors contributed equally

*Corresponding author: Bingcheng Wang. Department of Physiology and Biophysics, Case Western Reserve University, Cleveland, OH, USA

Received: January 03, 2025; Accepted: January 28, 2025; Published: January 30, 2025

Abstract

Overexpression of EphA2 receptor tyrosine kinase (RTK) in multiple human solid tumors is associated with poor prognosis. However, how it drives specific malignant processes remain elusive. Using metastatic human PCa specimens from two Rapid Autopsy Programs, we find selective upregulation of EphA2 protein in bone but not visceral metastases. Serine 897 phosphorylation that mediates oncogenic, ligand-independent noncanonical signaling by EphA2 was also upregulated in bone metastasis. Consistently, analysis of large human datasets shows that loss of ephrin-A1 ligand and gain of EphA2 expression are correlated with poor survival. Importantly, bone expresses little ephrin-A ligands relatively to all other tissues, providing uniquely permissive microenvironment to support noncanonical signaling by EphA2 on the disseminated cancer cells. Restoration of ephrin-A1 expression in PC-3, a cell line derived from bone metastasis deficient in ligand expression, profoundly changed global tyrosine phosphorylation profiles, reactivated the tumor suppressive canonical signaling, by EphA2 and inhibited tumor development in the bone. S897A mutation that ablates noncanonical signaling, suppressed PCa development. Our results demonstrate that loss of ephrin-A ligands elevates noncanonical signaling by the overexpressed EphA2 on PCa cells, which is maintained in osseous TME deficient in ligand expression and contributes to the strong bone tropism of PCa metastasis.

Introduction

Prostate cancer (PCa) is the most common non-skin cancer in men and is the second leading cause of cancer death in men within the United States [1]. While usually indolent or benign, a small fraction (5%) rapidly progress to malignant diseases [2,3]. PCa is initially responsive to androgen deprivation therapy (ADT) or castration. However, aggressive forms of the disease inevitably become resistant to this therapy [4-6], leading progressively to metastatic castration resistant PCa (mCRPC), a fraction of which further progress to neuroendocrine (NEPC) and double negative PCa (DNPC) where both androgen receptor (AR) and NEPC markers are lost. Since the approval of potent AR inhibitors, including enzalutamide and abiraterone, the clinical presentation of PCa subtypes has undergone dramatic shift. For example, the incidence of DNPC has increased nearly 4 folds in a Rapid Autopsy patients from 1998–2011 (5.4%) to 2012-2016 (23.3%) [7], concomitant with a drop in AR-positive disease, although the latter still constitutes majority of the CRPC patients. Consistently, chromatin profiling showed 27% to 37% of the patients treated with the potent AR inhibitors are AR-negative or -low [8]. Prostate cancer frequently metastasizes to bone with 70%–90% of patients having radiographically detectable skeletal involvement. Genetic studies show skeletal dissemination occurs early and takes a long time to cultivate [9]. However, despite recent progress, we still have very limited understanding of why PCa spreads to the bone so effectively early on. Clinically, bone metastases remain incurable and contribute significantly to patient morbidity and mortality worldwide. Discovery of molecular and cellular mechanisms behind PCa progression to skeletal metastasis is imperative to identifying new therapeutic targets and areas of intervention [10].

EphA2 receptor tyrosine kinase (RTK), a member of the Eph subfamily of RTKs, has been previously implicated in PCa. EphA2 is overexpressed in mCRPC, but not in early localized PCa tumors [11], and subsequent studies supported these findings [6,12]. We reported previously that EphA2 has dual opposing roles as both an oncogene and a tumor suppressor, and can switch between the roles dependent on binding of its ephrin-A ligands [13]. Ligand stimulation leads to EphA2 canonical signaling characterized by tyrosine kinase catalytic activation and inhibition of Ras/ERK [14], PI3K/Akt [13] and β 1 integrin-mediated signaling pathways [15], pointing to tumor suppressive roles. Genetic studies confirmed this notion, as EphA2 knockout mice displayed dramatically increased susceptibility to carcinogenesis [16]. In the absence of ligand, EphA2 becomes a target of AGC family serine/threonine kinases including Akt, RSK and PKA that phosphorylate serine 897 (pS897), an event that converts EphA2 from a tumor suppressor into an oncogenic proteins that promotes tumor cell migration, stemness, and development of drug resistance in multiple cancer types [13,17,18]. Molecularly, recent studies using the time-resolved live cell spectroscopy revealed that the EphA2 noncanonical signaling is enabled by the head-tail interaction between the ligand binding domain and the second fibronectin type II repeat of two adjacent receptors [19]. In PCa, EphA2 noncanonical signaling contributes to PCa cell migration in vitro and metastasis in vivo [20–24]. Despite these progresses, the molecular mechanisms and pathological significance of

EphA2 in mCRPC remain incompletely understood; even less is known whether EphA2 and its cognate ephrin-A ligands play a role in bone tropism of PCa metastasis.

Interestingly, Morrissey et al. show that ephrin-A1 was one of the top three genes lost in mCRPC, especially in bone metastases [25]. The loss of ephrin-A ligand expression and gain of EphA2 expression tilt the balance in favor of the pro-oncogenic, noncanonical signaling. However, whether EphA2 noncanonical signaling through pS897 is activated during PCa progression toward mCRPC in human diseases has yet to be documented, nor is it known if it contributes to metastatic PCa progression in vivo including its preferential bone colonization.

To fill this major gap, we interrogated the relationship of EphA2 signaling and the malignant progression of PCa. Using a combination of cell and animal models, public datasets, as well as human tissue samples from two Rapid Autopsy Programs, we found that EphA2 is dynamically upregulated during PCa progression to mCRPC concomitant with increased serine 897 phosphorylation, and loss of ephrin-A1 ligand. Importantly, we report EphA2 overexpression and pS897 signal in human bone metastatic specimens, demonstrating activation of EphA2 ligand-independent pro-oncogenic signaling, which was sustained in the bone milieu largely devoid of any ephrin-A ligand expression. Lastly, we show that PCa tumor growth is diminished by either disruption of non-canonical signaling with the S897A mutation, or restoration of ephrin-A1 expression in PC-3 cells, originally derived from bone metastasis and devoid of endogenous ephrin-A expression, blocked xenograft growth in the bone. Together our data establish a role of EphA2 in progression toward mCRPC wherein the increased EphA2 expression and decreased ligand enables abundance of ligand-independent signaling via S897phosphorylation of EphA2 [12], which is sustained in the ligand-low skeletal TME, leading to increased bone colonization.

Materials and Methods

Gene expression analysis from publicly available datasets

Expression of EPHA receptors and EFNA ligands as well as expression of AR, and KLK3 by human PCa cell lines was presented as log₂ transformed fragments per kilobase of transcript per million fragments mapped (FPKM). Gene expression information was obtained from a dataset accumulated by Smith R. et al. [29]. These data utilize human cell lines characterized as being castration resistant, androgen sensitive, or having an intermediate phenotype. Bulk RNA sequencing was performed as described in Smith R. et al. [29].

Data showing correlations of EPHA receptor expression to AR expression were acquired from 208 human metastatic PCa biopsies as part of the SU2C/PCF Dream Team published in PNAS 2019. Data points in the correlation plots represent mRNA expression z-scores relative to all samples. Statistical analyses of Pearson correlations presented were performed with GraphPad Prism 9. The mRNA expression dataset was accessed through cBioportal [26,27].

Patient survival Kaplan Meier plots were generated using data from both the SU2C/PCF Dream Team (PNAS, 2019.) and MSK (Cancer Cell, 2010). datasets. The SU2C/PCF Dream Team data-

set consists of at least 96.8 percent metastatic tissue samples, while the MSK dataset consists of 75.4 percent primary prostate tumor samples. In the SU2C/PCF data set EPHA2 mRNA expression is reported as z-scores relative to all samples. Our EphA2 “High” expressing group consisted of expression scores 1-2.5 and 0-0.25 and our EphA2 “Low” consisted of -1.75-0. In the MSK data set both EFNA1 and EPHA2 were separated into expression quartiles and the top 25 percent expressing samples were considered the “High” group, while all remaining samples were considered as “Low” expression. Logrank tests and plotting were performed with GraphPad Prism 9. The datasets were accessed through cBioportal [26,27].

EphrinA expression from non-tumor human tissues was exported from the Human Protein Atlas [28], and analyzed with GraphPad Prism 9 (Human Protein Atlas, <https://www.protein-atlas.org/>). Data presented consist of data from GTEx represented as normalized transcripts per million log10. Data normalization was performed previously by the Human Protein Atlas.

Tissue microarray

Human tissue microarray specimens were obtained through collaboration with the Pacific Northwest Prostate Cancer SPORE through Dr. Beatrice Knudsen, and Dr. Colm Morrissey. Of significant interest to us, they have constructed TMA from the bone and soft tissue metastases of PCa as part of the SPORE’s Rapid Autopsy Program. Rigorous quality control and patient documentation are in place for the tissue procurement. TMAs have been verified as suitable for IHC detection of multiple phospho-proteins, requisite for the studies proposed in this application.

Cell lines and reagents

PC-3, DU145, LNCap, CWR22R, and C4-2 cell lines were obtained from the American Type Culture Collection (ATCC, Manassas, VA). These cells were cultured in RPMI 1640 media supplemented with 10% fetal bovine serum, 10 mg/ml glutamine, 100 U/ml penicillin, and 0.1 mg/ml streptomycin. LAPC4 and LACP9 cells were obtained from Dean Tang with permission from Robert Reiter (UCLA) and cultured in Iscove’s Modified DMEM supplemented as above with addition of 1nM DHT. TRAMPC1 cells, obtained as a gift from Norman Greenberg, were cultured in DMEM supplemented with 5% fetal bovine serum 5% Nu serum, 10 mg/ml glutamine, 100 U/ml penicillin, 0.1 mg/ml streptomycin, and 10 nM dehydroepiandrosterone (DHEA). MPC3, MycCaP, and 293FT cells were cultured in DMEM supplemented similar to PC-3 cell culture. Cells were maintained in a humidified incubator at 37°C and 5% CO₂. All cell lines were routinely tested for mycoplasma contamination.

Ephrin-A1-Fc was produced as described previously [15]. Rabbit anti-pEphA/B antibody was raised against the conserved phosphopeptides in the juxtamembrane regions (Miao et al. 2009) [13]. Rabbit polyclonal pS897-EphA2 antibody was produced as described previously [13], as well as purchased Cell Signaling Technology (CST) (#6347S). Rabbit polyclonal anti-ephrin-A1 antibody was purchased from Santa Cruz Biotechnology (sc-911). Other antibodies were purchased as follows: Rabbit monoclonal anti-GAPDH (CST #2118S), rabbit monoclonal anti-pS473-Akt (CST #4060), rabbit polyclonal

anti-pErk1/pErk2 (CST #9101S), rabbit monoclonal anti-EphA2 (CST #6697S), rat monoclonal anti-EphA2-PE (R&D Systems FAB639P), rabbit monoclonal anti-AR (Abcam ab133273), rabbit polyclonal anti-pY772-EphA2 (CST #8244S), rabbit monoclonal anti-pY588-EphA2 (CST #12677S), mouse monoclonal anti-Tubulin (R&D Systems MAB9344), rabbit monoclonal anti-Akt1 (CST #2938), rabbit monoclonal anti-FAK (D2R2E) (CST #13009), rabbit monoclonal anti-pFAK-Y397 (CST #3283), mouse monoclonal anti-E-cadherin (BD 610181), rabbit monoclonal anti-N-cadherin (CST #13116), rabbit monoclonal anti-pSrc Family Y416 (D4964) (CST #6943), rabbit polyclonal c-Src (SRC2) Santa Cruz Biotechnology (sc-18), mouse monoclonal anti-pY99 Santa Cruz Biotechnology (sc-7020).

Goat anti-rabbit and goat anti-mouse secondary antibodies conjugated to horseradish peroxidase (HRP) were purchased from Santa Cruz Biotechnology (Santa Cruz, CA) and from Biorad (#1706515, and #1706516 respectively). For immunohistochemistry, mouse monoclonal anti-EphA2 was purchased from Millipore (Bedford, MA). Mouse monoclonal anti-tubulin was purchased from Sigma (Saint Louis, MO). Donkey anti-rabbit RedX conjugated secondary antibody was purchased from R&D Systems (Minneapolis, MN).

Cell lysate immunoblotting

Cells were cultured as described and lysate was collected when cells were subconfluent (~70% confluent). Media and cells were lysed in modified RIPA Buffer as described previously [15], and stored in loading buffer containing sodium dodecyl sulfate (SDS) and phosphatase inhibitors. Lysates were separated using the Bolt System (Life Technologies, Grand Island, NY) and 4-12% Bis-Tris Plus gradient gels, followed by transfer to PVDF membranes according to manufacturer’s instructions. Membranes were blocked for 1 hour at room temperature in 3% BSA in 0.05% TBS-T, followed by overnight incubation in appropriate primary antibodies. Cells were then washed in 0.05% TBS-T and incubated 1 hour at room temperature in appropriate secondary antibodies, followed by further washing and development with Luminol Reagent (Santa Cruz Biotechnology, Santa Cruz, CA).

Cell stimulations

Stimulations with ephrinA1-Fc ligand (EA1 or EA1-Fc) were done in 6 well corning cell culture plates following cell growth for 2 days, or until plates were approximately 70% confluent. Attached cells were treated with 2 µg/ml EA1-Fc for 0, 15 and 60 minutes without changing cell culture media.

For stimulations of PC-3 cells with FBS followed a 24 hour period of serum starvation, cells were exposed to either 10% FBS or 10% FBS plus EA1-Fc for a period of 1 hour prior to lysate collection.

Immunofluorescence staining

For immunofluorescence staining, cells were cultured on 10 mm square coverslips for 2 days, then stained as described previously [15]. Briefly, cells were fixed in 4% paraformaldehyde, followed by permeabilization with 0.5% NP-40 and blocking with Blocking Buffer (3% BSA, 2% goat serum, PBS). Cells were then washed in PBS, then 0.1% BSA/PBS and incubated with rabbit polyclonal anti-EphA2 antibody. Cells were then incubated with RedX-conjugated donkey anti-rabbit secondary an-

tibody, followed by mounting in Mounting Medium with DAPI (Vector Laboratories, Burlingame, CA). Staining was analyzed with a Leica Microsystems microscope and imaged using MetaMorph software (Leica Microsystems, Wetzlar, Germany).

Animal models and subcutaneous injections

Syngeneic animal experiments were completed with C57Bl/6J and FVB/NJ mice purchased from Jackson Laboratory (000664). All xenograft models were completed with nude mice bred at the Athymic Mice Core at the Case Comprehensive Cancer Center. All animal husbandry and procedures were approved by the Institutional Animal Care and Use Committee (IACUC) at Case Western Reserve University. Subcutaneous injections were completed by resuspension of cells in endotoxin-free PBS and injection of both hind flanks of the mouse with 100 μ l solution. All animals were monitored 24 hours post-injection as well as twice a week post evidence of tumor formation.

Serial in vivo passage of murine PCa cells in syngeneic host

Parental TRAMPC1 cells were injected subcutaneously into syngeneic C57Bl/6J mice at 5.0×10^6 cells per flank. Post 80 days of tumor formation tumors were excised and dissociated in Collagenase IV (Sigma-Aldrich #C4-22-1G) containing 10 μ M Y27632 dihydrochloride (AdooQ Bioscience #A21448). Approximately 0.5 g of tumor tissue was processed with the Milteny OctoDissociater. Digested samples were passed through a 70 μ M cell strainer and washed with 8 ml of DMEM containing 10% FBS. Cells were plated under treatment with fungicide and tetracycline to prevent contamination. After up to 5 passages ex vivo and at least 1 freeze thaw cycle, the cells were checked for mycoplasma contamination, and then injected into syngeneic hosts subcutaneously at 5.0×10^6 cells per flank. These injected cells were termed "in vivo 1," (TRAMPC1 IV1) as they had been through a single round of in vivo tumor growth.

MycCaP and MPC3 cells were selected in vivo in the same manner. MycCaP cells were injected at 0.7×10^6 cells per flank for 21 days, and MPC3 cells were injected at 2.0×10^6 cells per flank for 33 days. MycCaP and MPC3 cells were injected into syngeneic FVB/NJ and C57Bl/6J mice respectively.

Live cell staining and cell sorting

MPC3 cell populations from every time point during the process of in vivo selection in syngeneic host (Parent, IV1, IV2), were subjected to live cell staining of EphA2 with EphA2-PE (anti-mEphA2 PE conjugated R&D Systems #FAB639P). Flow cytometry was completed using the Sony MA900. The mean fluorescence intensity was recorded for each iteration for a minimum of 50,000 cells.

Parental TRAMPC1 cells were subjected to fluorescence-activated cell sorting (FACS) using EphA2-PE antibody and the Sony MA900 sorter which allowed isolation of 30% of the cells with the highest EphA2 expression, and 30% of cells with the lowest EphA2 expression.

Xenografts models

PC-3 and C4-2 cells were xenografted subcutaneously onto nude mice in the hind flanks. Cells were prepared in Corning 10 cm tissue culture plates until approximately 70% confluent. Cells were counted, washed with PBS, and mixed with PBS

(tested to be endotoxin free). 1.3×10^6 cells were injected into each flank and monitored for a period of 50 days.

Intratibial injection

PC-3 cells expressing firefly luciferase and either a vector control, or lenti EphrinA1 expression vector were delivered intratibially using a 28g, 1/2 inch needle under the patella, through the middle of patellar ligament, and into the anterior intercondylar area in top of the tibia. 2.0×10^5 cells were delivered in 20 μ l of PBS at an approximate rate of 5 μ l/second. Upon imaging mice were administered 200 μ l of 1.25 mg/ml D-Luciferin by intraperitoneal injection (IP) and anesthetized 5 minutes post injection with 1-5 percent isoflurane then imaged using the IVIS Spectrum Bioluminescence Imager. At Week 6, the tibia with PC-3 cell injection were also imaged by planar X-ray to examine bone losses.

Results

EphA2 is overexpressed in mCRPC cell lines in vitro and in bone metastasis specimens of human patients in vivo. To explore the pathological roles of EphA2 in the late stage metastatic PCa, we first analyzed gene expression from public bulk RNA sequencing data of human PCa cell lines [29], and discovered that castration resistant cell lines exhibited overexpression of EphA2 compared to androgen sensitive cell lines, which is consistent with earlier reports of increased EphA2 expression in human metastatic castration resistant specimens (mCRPC) [30], (Figure 1A). This is inversely correlated with expression status of AR and KLK3, a downstream target of AR encoding prostate specific antigen (PSA). Immunoblot analysis confirmed the low levels of EphA2 expression in androgen sensitive cell lines, whereas it is upregulated in metastatic castration resistant cells, particularly PC-3 cells derived from bone metastasis that have recently become a model for late stage DNPC (Figure 1B) [6,31,32]. This finding was further supported by immunofluorescence staining of EphA2, where it was readily detected in castration resistant DU145 and PC-3 cells, but weakly detected in androgen sensitive LNCaP and CWR22R cells (Figure 1C). The androgen sensitive LAPC4 are an exception and displays moderate mRNA and protein expression (Figure 1A, B). Serine 897 phosphorylation (pS897) that demarcates activation of the oncogenic noncanonical signaling is upregulated in metastatic PC3 and DU145 cells, but is absent from androgen sensitive cells, including LAPC4 cells despite moderate EphA2 expression.

To further confirm EphA2 overexpression in late-stage human PCa tissues in pathologically relevant settings, we probed a panel of lysates prepared from primary and metastatic PCa tissues harvested in the University of Michigan Rapid Autopsy Program [33]. Interestingly, we found that EphA2 is more highly expressed in bone metastatic tissues compared to tissues from benign prostate, primary tumors, or lymph node metastases (Figure 1D).

Next, we investigated whether other members of the EphA receptors were similarly regulated in PCa. Surprisingly, among the 9 mammalian EphA receptors, EphA2 was the only one overexpressed in castration resistant cell lines in the Smith dataset [29], (Figure S1A) indicating that EphA2 is the predominantly expressed EphA receptor in castration resistant PCa. Consis-

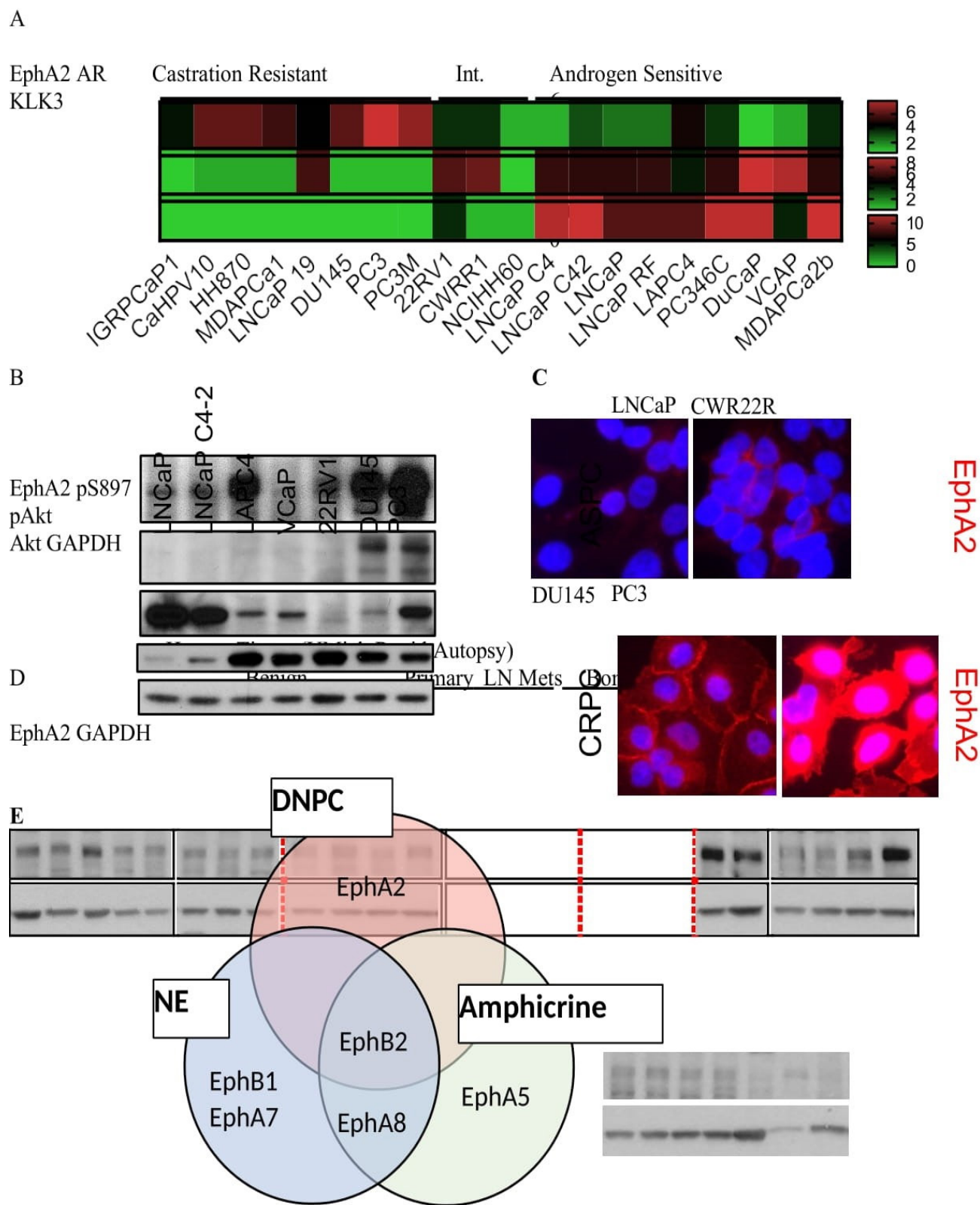
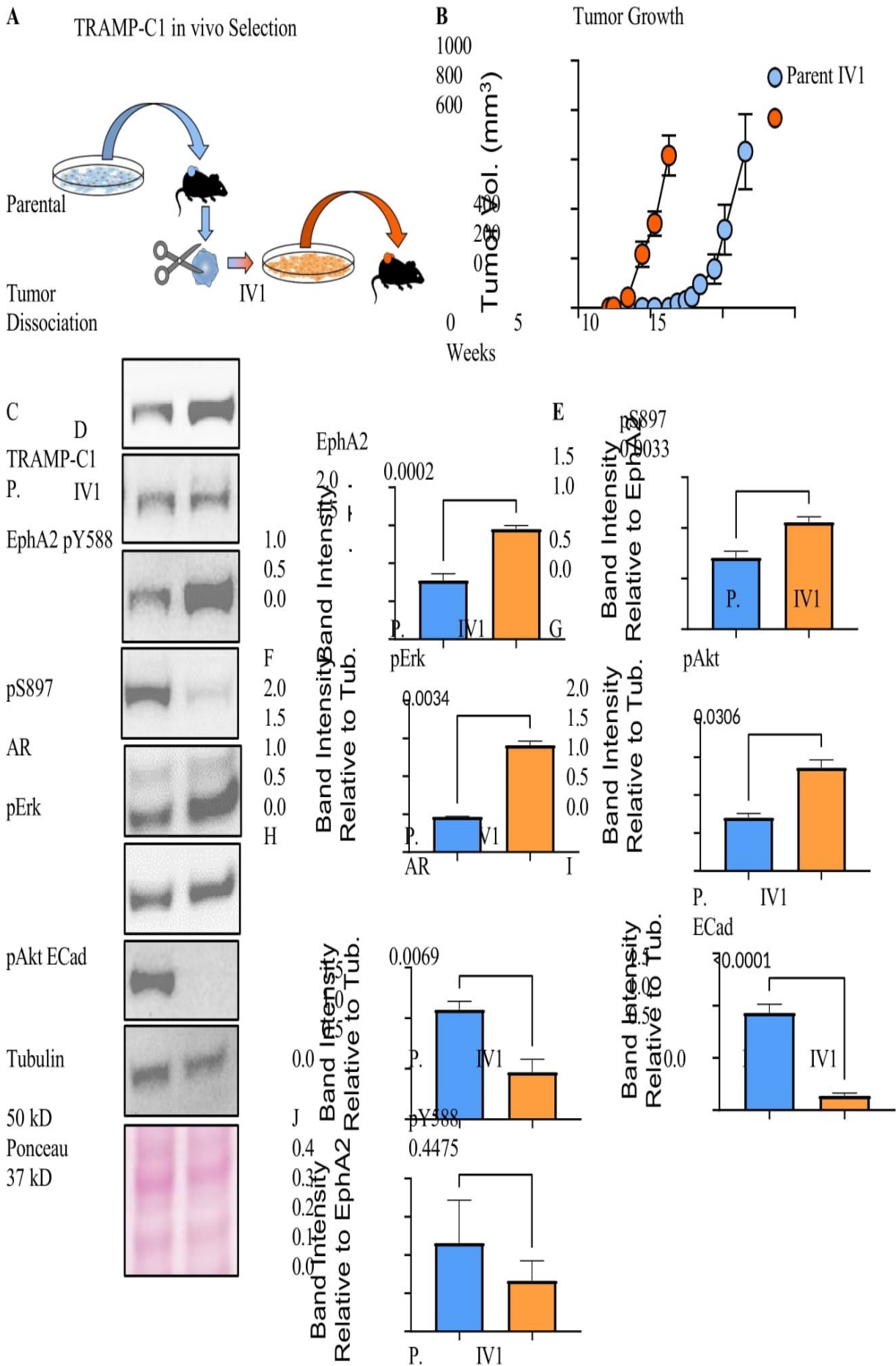


Figure 1. EphA2 is Overexpressed in Castration Resistant and Metastatic Prostate Cancer A) Analysis of log₂ transformed FPKM gene expression values extracted from bulk RNA seq published previously (Smith R. et al. Scientific Reports 2020) shows high EphA2 expression in castration resistant, commercially available human PCa cell lines. B) Immunoblot characterization of select human PCa cell lines show increased EphA2 expression and S897 phosphorylation in mCRPC derived cell lines. C) EphA2 expression in representative human prostate cancer cell lines. D) Lysate of human prostate cancer tissues reveal increased expression of EphA2 in bone metastasis samples. Lysates were prepared from micro-dissected human prostate cancer tissues under the Rapid Autopsy Program at the Univ. Mich. PCa SPORE. E) Expression of Eph receptors in in metastatic neuroendocrine (NE), amphotericin (amphi) and double negative PCa (DNPC) relative AR positive PCa. RNA data from Labrecque et al. reference #6.



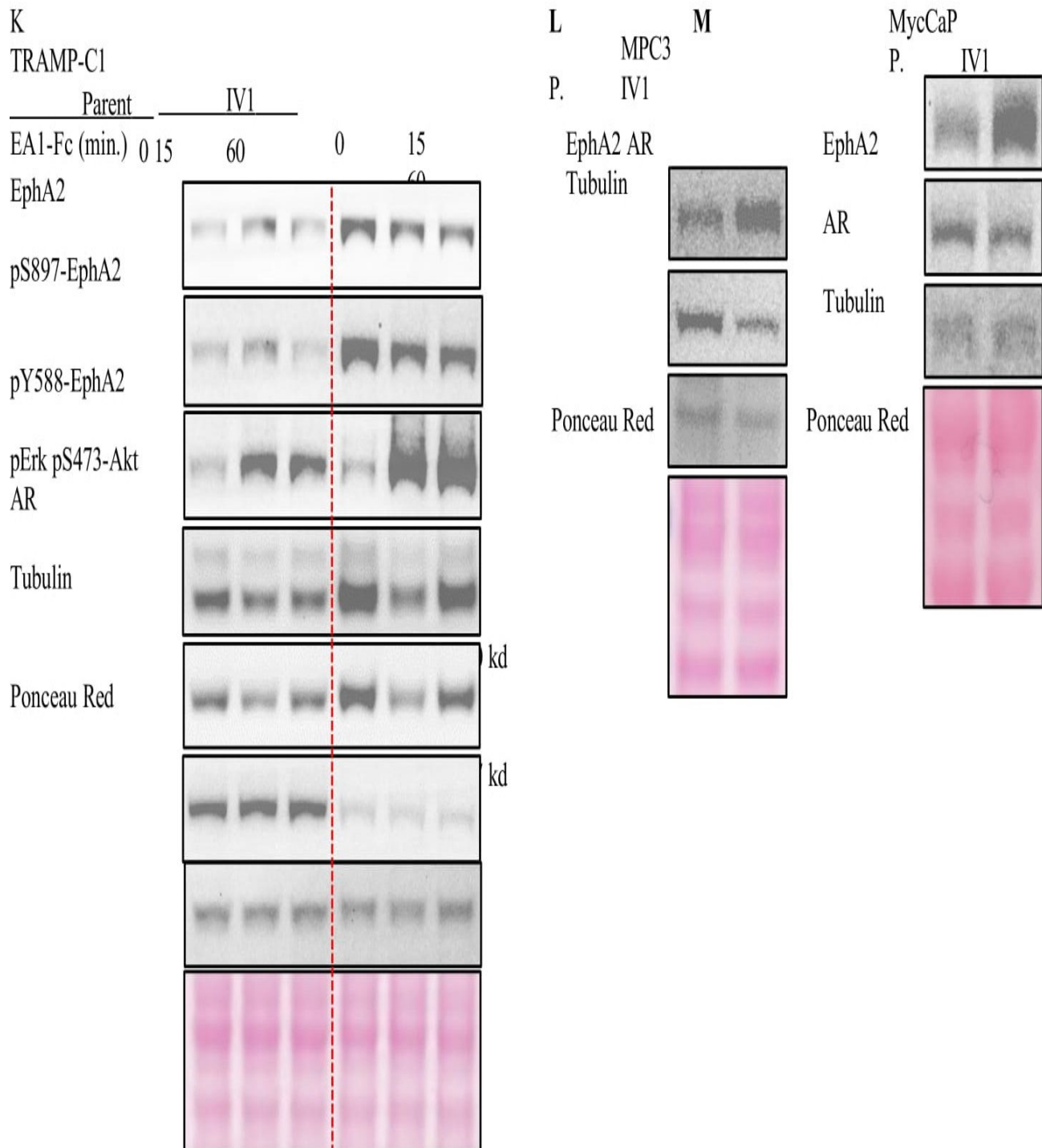


Figure 2. EphA2 is upregulated following in vivo selection for enhanced tumorigenicity. A) Diagram depicting the serial propagation of TRAMP-C1 cells in syngeneic mice to select for cells with increased tumorigenic capacity. B) The in vivo selection of cells resulted in accelerated tumor growth and reduced latency. C) Immunoblot analyses of the in vivo selected (IV1) and the parental TRAMP-C1 cells using the indicated antibodies. D,E,F,G,H,I,J) Quantification of relative band intensity (n = 4). All bands normalized to tubulin, except for pY588 and pS897 which are normalized to total EphA2 expression. K) Immunoblot of TRAMP-C1 parental and IV1 cells after stimulation with Ephrin-A1-Fc ligand for the indicated times. L,M) MPC3 and MycCaP cells were propagated in syngeneic C57Bl/6 and FVB mice, respectively. Lysates of the parental and the in vivo selected cells (IV1) were subject to immunoblot using the indicated antibodies.

tently, among all the mammalian EphA receptors, EphA2 is the only receptor showing negative correlation to AR expression in human metastatic biopsies (Figure S1B). Our previous study using molecular profiling has led to the stratification of treatment-refractory mCRPC into diverse phenotypes. Analysis of the same dataset reveal that EphA2 overexpression aggregates in the DNPC relative to ARPC among the mCRPC (Figure 1E).

EphA2 is upregulated during malignant progression of PCa in vivo

To analyze the dynamics of EphA2 expression during PCa progression, we modeled increasing malignancy by serially passaging murine PCa cell lines in syngeneic host in vivo. We selected the TRAMP-C1 cell line derived from prostate adenocarcinoma induced by SV40 T antigen in C57Bl/6J mice [34,35]. Cells were injected subcutaneously; the resulting tumors were dissociated and cells were isolated for culture (Figure 2A). When re-grafted into new mice, the selected cells, termed in vivo 1 (IV1), exhibited accelerated tumor development compared to the parental TRAMP-C1 cells with five weeks of shortened latency (Figure 2B). Interestingly, the IV1 cells show significantly elevated expression of EphA2 (Figure 2C,D). The basal level of pS897 was also increased (Figure 2C,E), suggesting activation of pro-oncogenic noncanonical signaling by EphA2. The levels of pAkt and pERK, known upstream kinases that directly and indirectly phosphorylate S897, respectively, were also significantly increased (Figure 2C,F,G). In keeping with the inverse correlation between AR and EphA2 expression in human PCa cell lines, the more malignant TRAMP-C1 IV1 cells also showed loss of androgen receptor (Figure 2C,H). Here AR loss serves as a marker of progression toward CRPC coinciding with increased EphA2 expression, however, our investigation did not reveal a direct relationship between AR and EphA2 expression. Expression of E-cadherin, an epithelial cell marker highly expressed in parental cells (Figure 2C,I), is reduced to nearly undetectable level, consistent with increased malignancy of IV1 cells associated with epithelial-mesenchymal transition (EMT). The basal catalytic activation of EphA2 tyrosine kinase activity, as measured by pY588 did not change much (Figure 2C,J) despite higher EphA2 expression, suggesting diminished canonical signaling.

As we have shown previously [13], stimulation with exogenous ephrin-A1-Fc ligand caused tyrosine kinase activation, leading to inhibition of ERK and Akt activities (Figure 2K). S897 phosphorylation associated with noncanonical pro-oncogenic function of EphA2 was decreased by the ligand treatment. Therefore, the overexpressed EphA2 retains its intrinsic tumor suppressive function upon ligand stimulation.

To further validate the correlation between EphA2 expression and elevated pS897, pERK and pAkt, parental TRAMP-C1 cells were sorted into high and low EphA2 expressing populations. The high EphA2 expressing cells showed a higher basal level of S897, Akt and Erk phosphorylation, and were highly responsive to ligand stimulation (Figure S2A).

Next, we examined whether the upregulation of EphA2 following in vivo selection for malignant cells can be extrapolated to other syngeneic murine PCa models. MPC3 and MycCaP

PCa cell lines are derived from prostate-targeted co-deletion of PTEN and Trp53 and overexpression of Myc on C57Bl/6J and FVB background, respectively [36,37]. They were subjected to the same selection procedures in syngeneic mice (Figure 2A). Similar to TRAMP-C1, MPC3 and MycCaP cells selected in vivo exhibited increased EphA2 expression (Figure 2L,M). There also marked reduction of AR in MPC3 cells, while only a milder reduction was observed in MycCaP cells, possibly due to the very high basal level AR expression in these cells. Moreover, MPC3 cells subjected to iterative rounds of in vivo selection exhibited progressive increase in EphA2 expression (Figure S2B). Taken together, EphA2 expression and oncogenic signaling are increased concomitant with the loss of AR expression following in vivo selection for more malignant phenotype.

Bone metastases show preferential EphA2 overexpression and activation of noncanonical signaling

To investigate the pathological relevance of noncanonical signaling of EphA2 in human PCa, we obtained human prostate cancer tissue microarray (TMA) established by the Rapid Autopsy Program of the Pacific Northwestern Prostate Cancer Spore and stained them for pS897- and total EphA2. The TMA contains primary tumors as well as metastases to the lymph node and bone metastases, as well as soft tissue metastasis to the liver. Consistent with the biochemical analysis of tumor lysates from the Rapid Autopsy Program of University of Michigan PCa SPORE (Figure 1D), significantly higher EphA2 expression was detected in bone metastasis than the primary PCa or metastasis to the lymph and liver (Figure 3A, a-h and Figure 3B). Furthermore, bone metastatic tumor samples exhibited significantly elevated EphA2-pS897 staining compared to primary PCa and metastases to the LN and liver (Figure 3A, i-p and Figure 3C), demonstrating selective upregulation of pro-oncogenic, noncanonical signaling by EphA2 in bone metastasis relative to primary tumors and visceral metastases. Of note, we could not detect pS897 in the PCa tissue lysates used in Figure 1D, possibly due to the highly labile nature of the phosphoserine signals that were lost during lysate preparation and/or storage. Tissues for TMA were immediately fixed after harvesting and are more likely to retain pS897 signals. Confirming the biochemical (Figure 1D) and IHC results (Figure 3A), analysis of the SU2C/PCF dataset revealed significantly higher EphA2 expression in bone metastases compared to all other metastatic sites (Figure 3D). More importantly, higher EphA2 expression is correlated with worse survival among patients with bone metastasis (Figure 3E), whereas no such correlation was observed when all metastatic sites were included in the analysis (Figure S3A), nor was there such a correlation among primary PCa patients (Figure S3B).

Most bone metastasis specimens came from patients with mCRPC. To test how acquisition of castration resistance impacts EphA2 noncanonical signaling, we used LAPC9 human prostate cancer model that is derived bone metastasis and can be propagated in vivo as xenograft in immune deficient mice. As shown in Figure S3C,D,E, LAPC9 cells derived from the castrated host showed increased pS897 compared with androgen sensitive parental cells, as evidenced by both immunoblot and IHC staining. In sum, these data suggest that PCa metastases to the bone are associated with overexpression of EphA2 and activation of non-

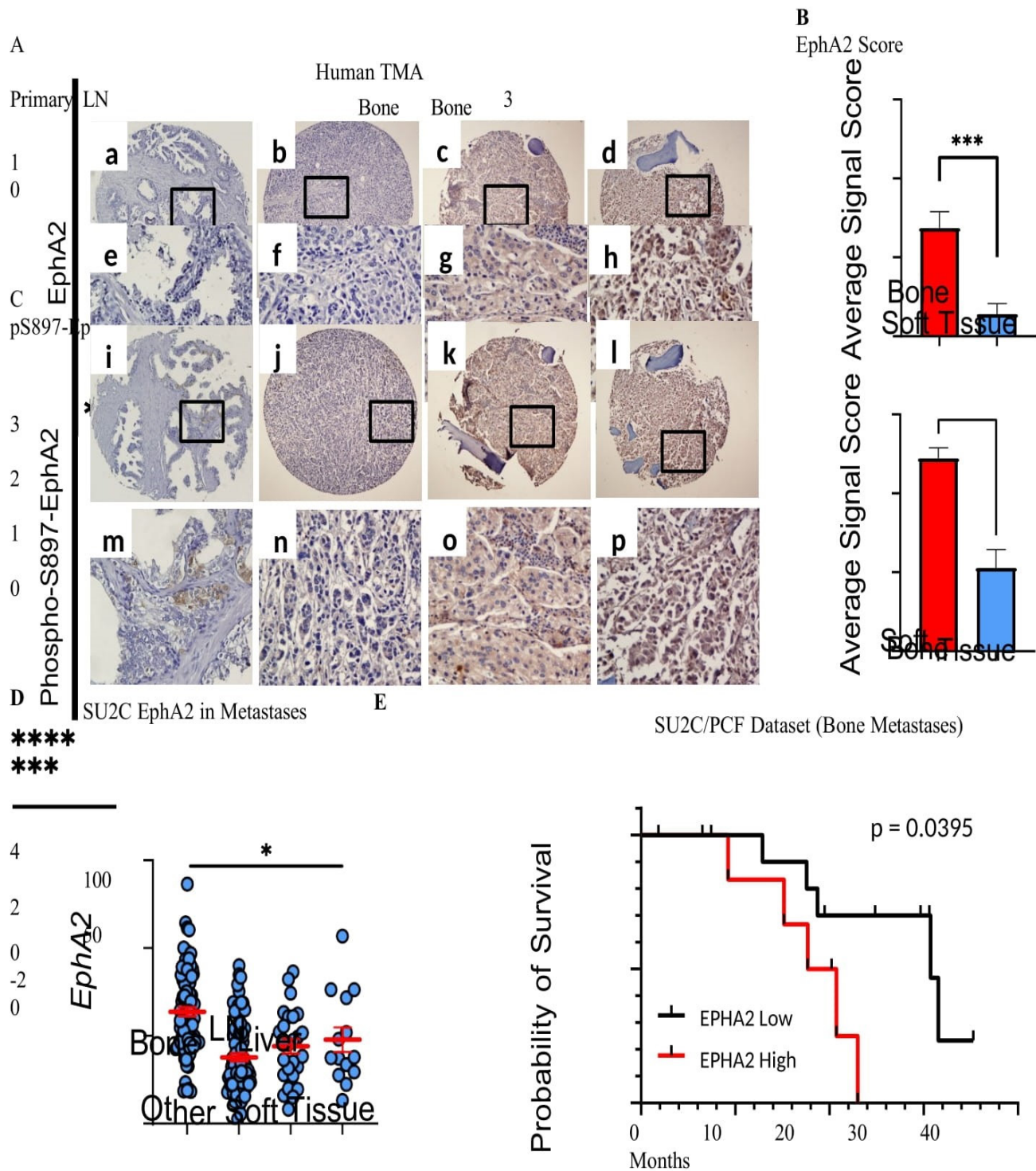


Figure 3. Differential overexpression and activation of noncanonical signaling of EphA2 in bone metastases. A) Immunohistochemical (IHC) analyses of tissue microarray (TMA) prepared from primary, lymph node metastatic (LN), and bone metastatic human PCa tissues from the Rapid Autopsy Program of the Pacific Northwest PCa SPORE spotted. B and C) The relative IHC staining strengths of EphA2 and pS897- EphA2 on TMA was scored using 0-3 scale (0, absent; 1, weak; 2, moderate; 3, strong) . Data consists of 27 bone metastatic samples, and 18 soft tissue samples including 10 lymph node, 5 liver, and 3 lung metastatic samples. Comparisons were made using an unpaired t-test (B, $p = 0.0003$ C, $p < 0.0001$) D) mRNA expression analysis of human PCa metastatic biopsies revealed that bone metastases have the highest EphA2 expression compared to other sites of disease dissemination. Data from 208 samples from the SU2C/PCF Dream Team. mRNA Expression z-scores relative to all samples (log FPKM Capture) accessed via cBioportal. E) Kaplan-Meier curve of patients with bone metastases according to the levels of EphA2 expression.

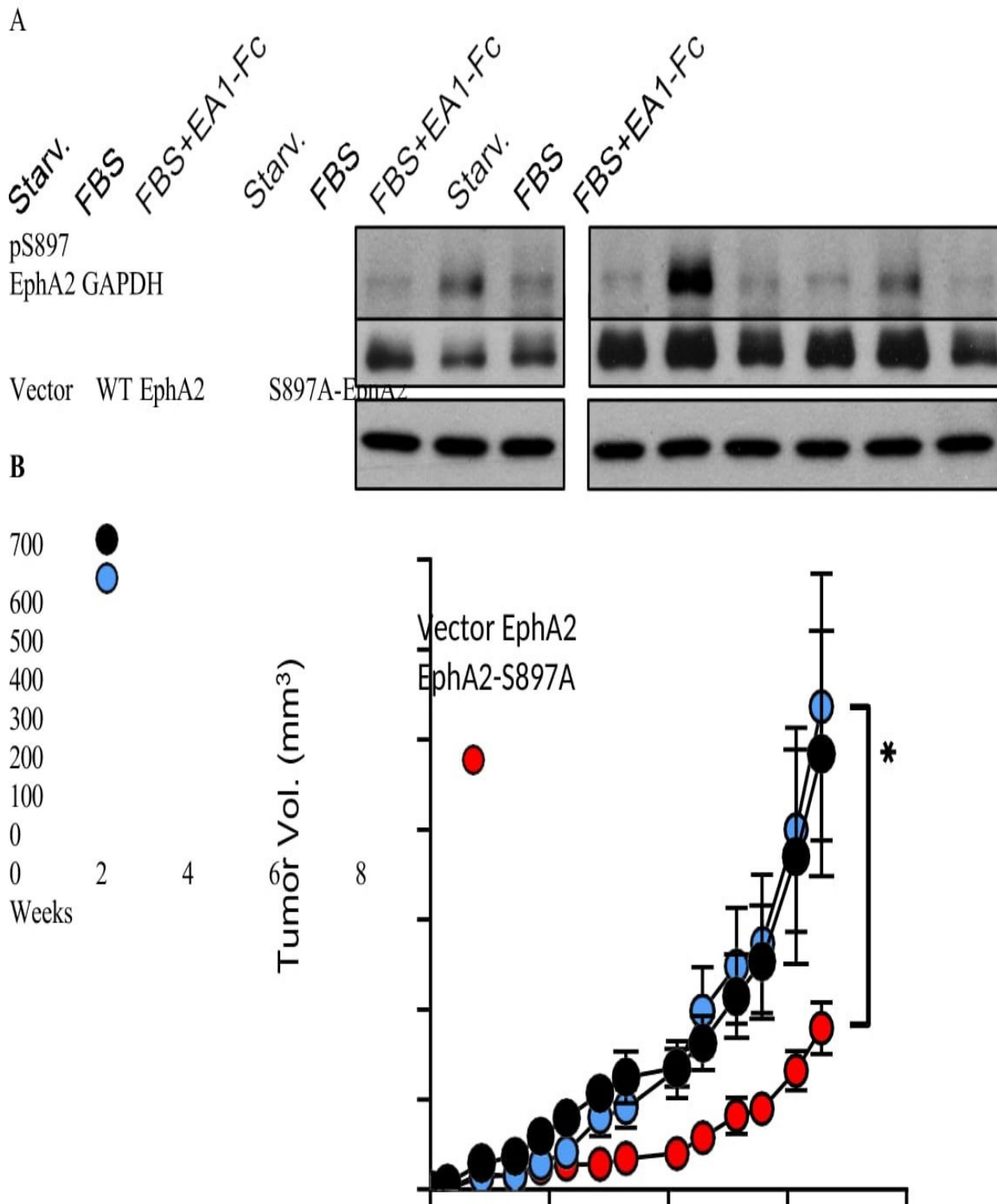


Figure 4. S897A mutation that disrupts the oncogenic noncanonical signaling resulted in diminished tumor development. A) Immunoblot analysis of PC3 cells transduced with lentivirus to express WT-EphA2 or S897A-EphA2. Empty vector-transduced cells were used as control. Cells were starved for 24 hours in serum-free medium and stimulated with either FBS alone or FBS together with ephrin-A1-Fc. B) PC3 cells overexpressing WT-EphA2 or S897A-EphA2 mutant were xenografted subcutaneously into nude mice (n = 10 per group). Vector alone cells were used as control. Comparison between WT-EphA2 and S897A-EphA2 made with an unpaired t-test at day 46 post-injection (p = 0.0402).

EphrinA Expression in Healthy Tissue

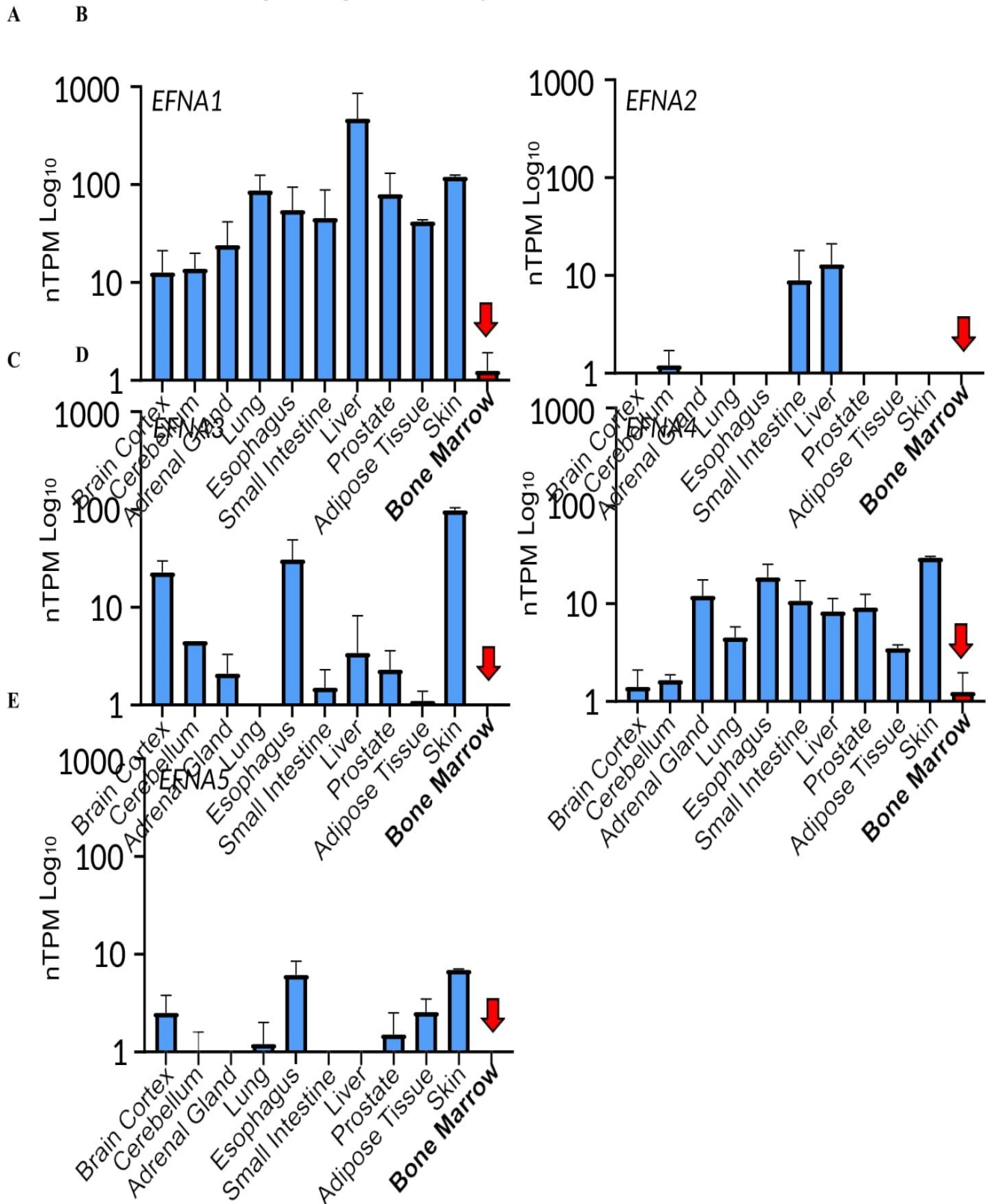


Figure 5. Undetectable or very low expression of all five EFNA genes in the bone microenvironment. A-E) EFNA1,2,3,4,5 expression across human tissues. Data was collected from Human Protein Atlas. F) qPCR analysis of bone marrow samples from four healthy human donors; 22Rv1 cells were used as control.

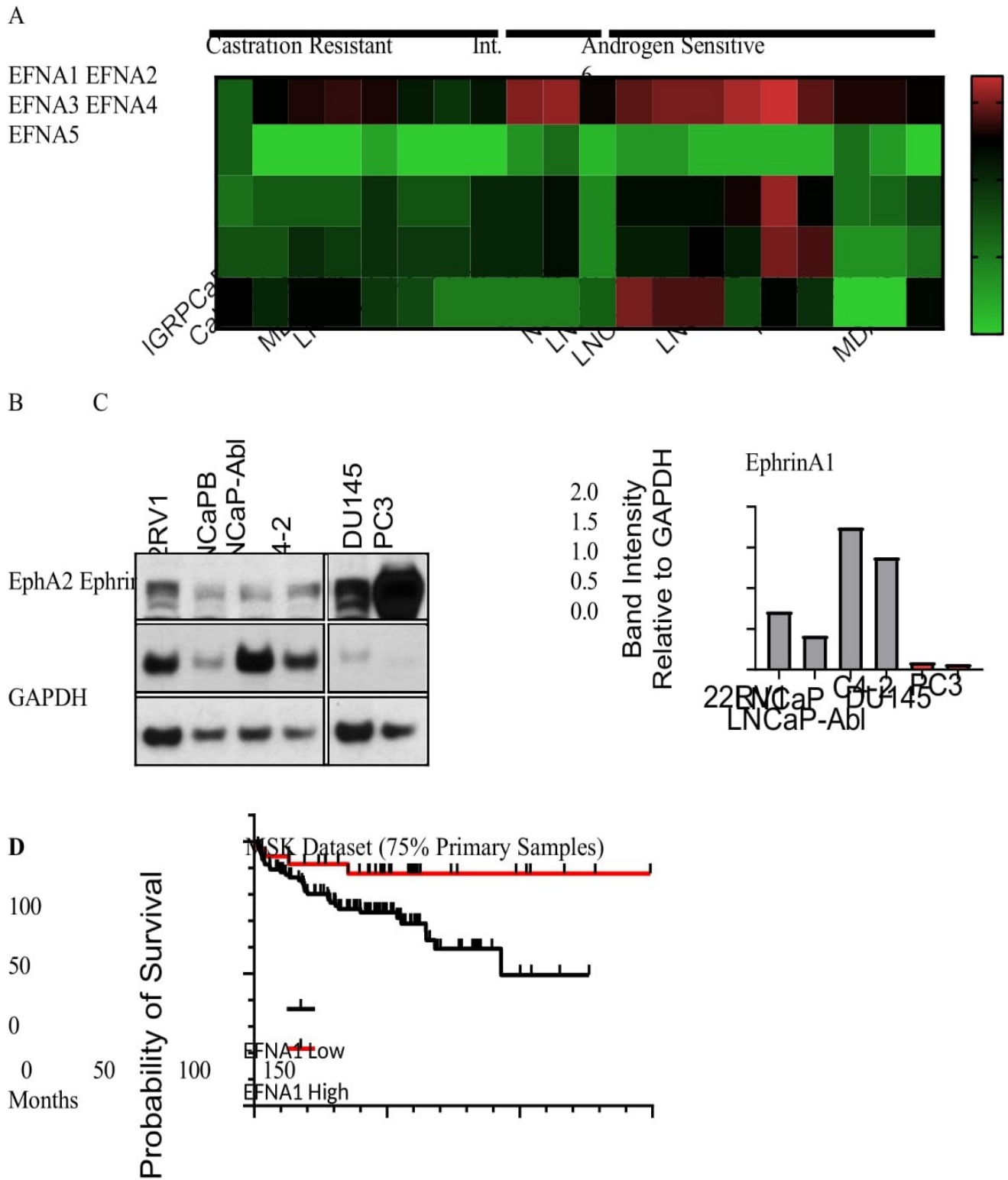


Figure 6. Ephrin-A1 is lost in mCRPC. A) Analysis of log2 transformed FPKM gene expression values extracted from bulk RNA seq published previously (Smith R. et al. Scientific Reports 2020) showing low Efn1-5 gene expression in commercially available castration resistant and androgen sensitive human PCa cell lines. B) Immunoblot characterization of select PCa cell lines reveals simultaneous high EphA2 expression and low EphrinA1 expression in metastatic castration resistant cells compared with androgen sensitive cells. C) Quantitative analysis of data in (B). D) Kaplan-Meier survival curve from the MSK dataset (Cancer Cell 2010). Samples were aggregated into the top 25 percent EFNA1 expressing (EFNA1 High), and lower 75 percent EFNA1 expressing (EFNA1 Low). Data were accessed via cBioportal.

canonical signaling, which is correlated with worse prognosis of the patients.

Disruption of noncanonical pro-oncogenic signaling via S897A mutation suppresses growth of PCa xenografts

To investigate the pathological relevance of EphA2 noncanonical signaling through S897 phosphorylation in PCa, we expressed S897A mutant EphA2 that abolishes noncanonical signaling in PC-3 cells. WT EphA2 was used as control, and both were expressed at similar levels (Figure 4A). Upon serum stimulation of starved cells, we observed strong induction of pS897 on WT EphA2. S897A-EphA2 cells had pS897 level that was comparable to vector control cells, suggesting the weak signal likely originated from the endogenous EphA2. Upon implantation into nude mice, PC-3 cells expressing S897A-EphA2 mutant exhibited significantly diminished tumor development compared to either the WT-EphA2, or vector expressing tumors (Figure 4B).

Next, we expressed WT or S897A-EphA2 in C4-2, an androgen insensitive human PCa cancer cell line derived from androgen-sensitive LNCaP. Like LNCaP, C4-2 cells express very low endogenous EphA2 (Figure 1A,B). Overexpression of WT EphA2 significantly promoted C4-2 xenograft tumor development, and the effect was diminished by S897A mutation (Figure S4A,B), indicating the requisite role of serine 897 phosphorylation in promoting tumorigenesis by EphA2.

Lack of ligand expression in the bone provides a permissive milieu for PCa metastasis

PCa metastasis is known to have strong bone tropisms. In the castration-resistant setting, 70%–90% of patients have radiographically detectable skeletal involvement [38–40]. The selective upregulation of EphA2 expression and noncanonical signaling in skeletal metastases suggests a potential role in the bone tropism. One of the best characterized functions of Eph receptors is the repulsion of migrating cells upon contact with ligand-presenting cells. This prompted us to examine the expression of ephrin-A ligands in the bone microenvironment. Strikingly, analysis of the Human Protein Atlas shows undetectable or very low expression of all five mammalian EFNA genes in the bone, which contrasts with all other tissues examined that have high EFNA1 expression and variable expression of the other four EFNA genes (Figure 5A–E). To further validate the observation, we obtained human bone marrows from four normal donors. qPCR analysis showed undetectable or very low expression of the five EFNA genes in all four bone marrow specimens relative to 22Rv1 human prostate cancer cell line with varying expression of EFNAs (Figure 5F). The absence of ephrin-As in the bone microenvironment creates a highly permissive microenvironment, as PCa cells presenting abundant EphA2 on the surface can home to the bone without being repulsed by the ligands on the skeletal cells. Moreover, the dearth of ephrin-A ligands in bone milieu together with their lack of expression on mCRPC cells (see below) also helps sustain the ligand-independent noncanonical signaling by EphA2 to promote PCa invasion and growth in the bone.

Ephrin-A1 expression is lost in mCRPC

The duality of EphA2 as a tumor suppressor gene and as an

oncogene is dictated by the presence and absence of the ephrin-A ligands, respectively. While the lack of the ephrin-A ligands in the bone marrow provides a permissive milieu, the ephrin-A ligands expressed on tumor cells can interact with EphA2 on adjacent cancer or stromal cells to trigger receptor-ligand interactions in trans and initiate tumor suppressive canonical signaling. Conversely, loss of ligand can facilitate pro-oncogenic EphA2 noncanonical signaling. Previous studies using mCRPC from rapid tissue acquisition necropsy show that EFNA1 is one of three genes whose expression was significantly reduced in bone metastases compared with primary tumors and lymph node or liver metastasis [25]. Consistently, we observe a low mRNA expression of all five EFNA genes across multiple castration resistant human PCa cell lines compared to androgen sensitive cells (Figure 6A). EFNA1 gene is widely expressed in all androgen sensitive cell lines followed by EFNA [3–5]. Immunoblot results confirmed the loss of ephrin-A1 expression in PC-3 and DU-145 CRPC cells compared with androgen sensitive cell lines (Figure 6B,C). Moreover, analysis of the MSK database (Cancer Cell, 2010) showed that low EFNA1 expression is associated with worse patient survival (Figure 6D). The EphA2 overexpressing and ephrin-A deficient prostate cancer cells can be preferentially selected in the bone as described above.

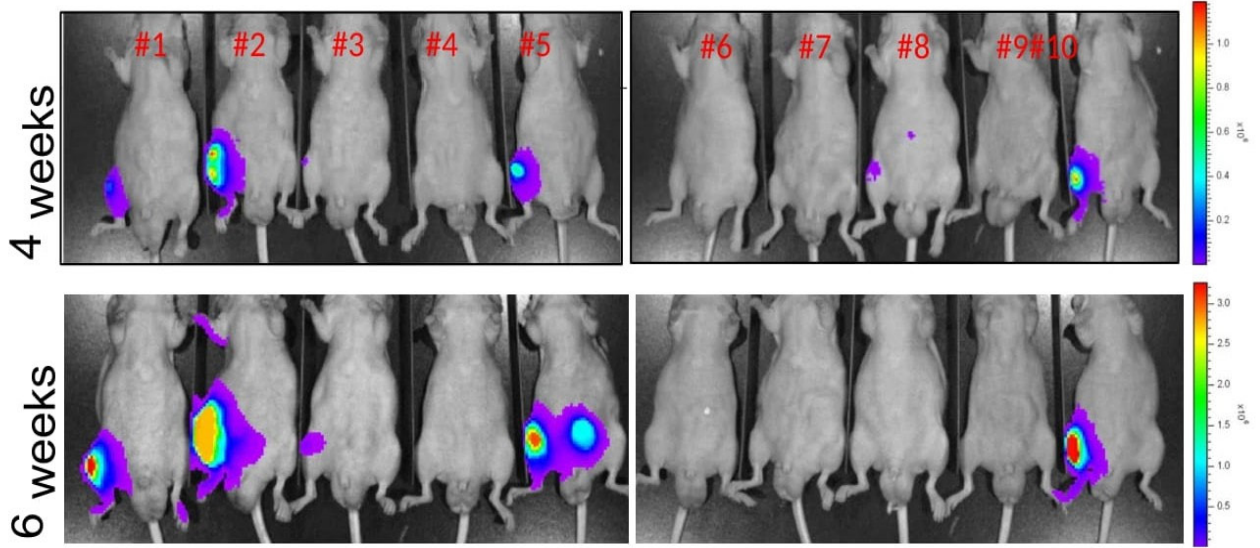
Restoration of EFNA1 expression in PC-3 cells suppresses oncogenic noncanonical signaling by EphA2 and reduces tumor development

The results above suggest that the loss of ephrin-A1 expression and ensuing activation of non-canonical signaling by the overexpressed EphA2 may contribute to malignant progression of PCa. To directly test this hypothesis, we used a lentiviral vector to re-introduce EFNA1 expression into PC-3 cells that are originally derived from a bone metastasis and have little expression of the five EFNA genes. As shown in Figure 7A, restoration of ephrin-A1 resulted in dramatic reduction in the total level of EphA2, likely due to EphA2 activation by ligand presented in trans on adjacent cells, leading to endocytosis and proteolytic degradation of the receptor. Ephrin-A1 re-expression also led to proportionally stronger basal tyrosine phosphorylation in the juxtamembrane domain (pY588) and reduced pS897 (Figure 6B,C), which is associated with canonical and noncanonical signaling of EphA2, respectively.

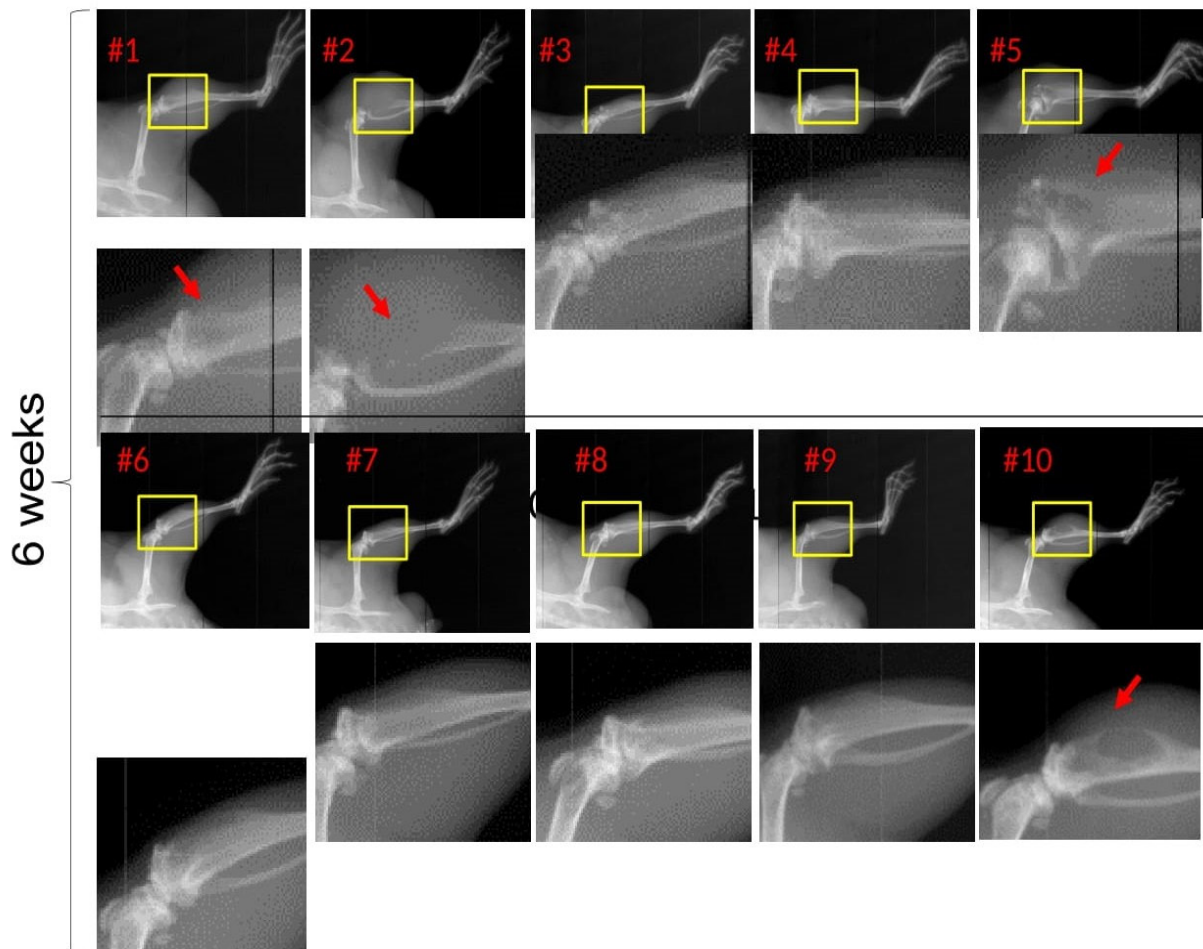
As reported previously [13,14], stimulation of control cells with recombinant ephrin-A1-Fc led to potent activation of canonical signaling characterized by EphA2 tyrosine phosphorylation and suppression of both ERK and Akt (Figure 7D). Restoration of ephrin-A1 in PC-3 cells led to diminished basal ERK activities (Figure 7D, lanes 1 vs. 4). The basal activities of Akt, on the other hand, remained unchanged. Despite much lower basal level of EphA2 on ephrin-A1-restored cells, it remained responsive to exogenous ligand stimulation, leading to inhibition of Akt (Figure 7D) and pS897 (Figure S5).

To explore how ephrin-A1 restoration effects global changes in cell signaling machinery, we probed whole cell lysates for overall pY profile, utilizing an anti-pY antibody (PY99) that recognized most tyrosine-phosphorylated proteins. Stable restoration of ephrin-A1 caused a profound reduction in total pY

pLenti PC3-Ephrin-A1



PC3-pLenti



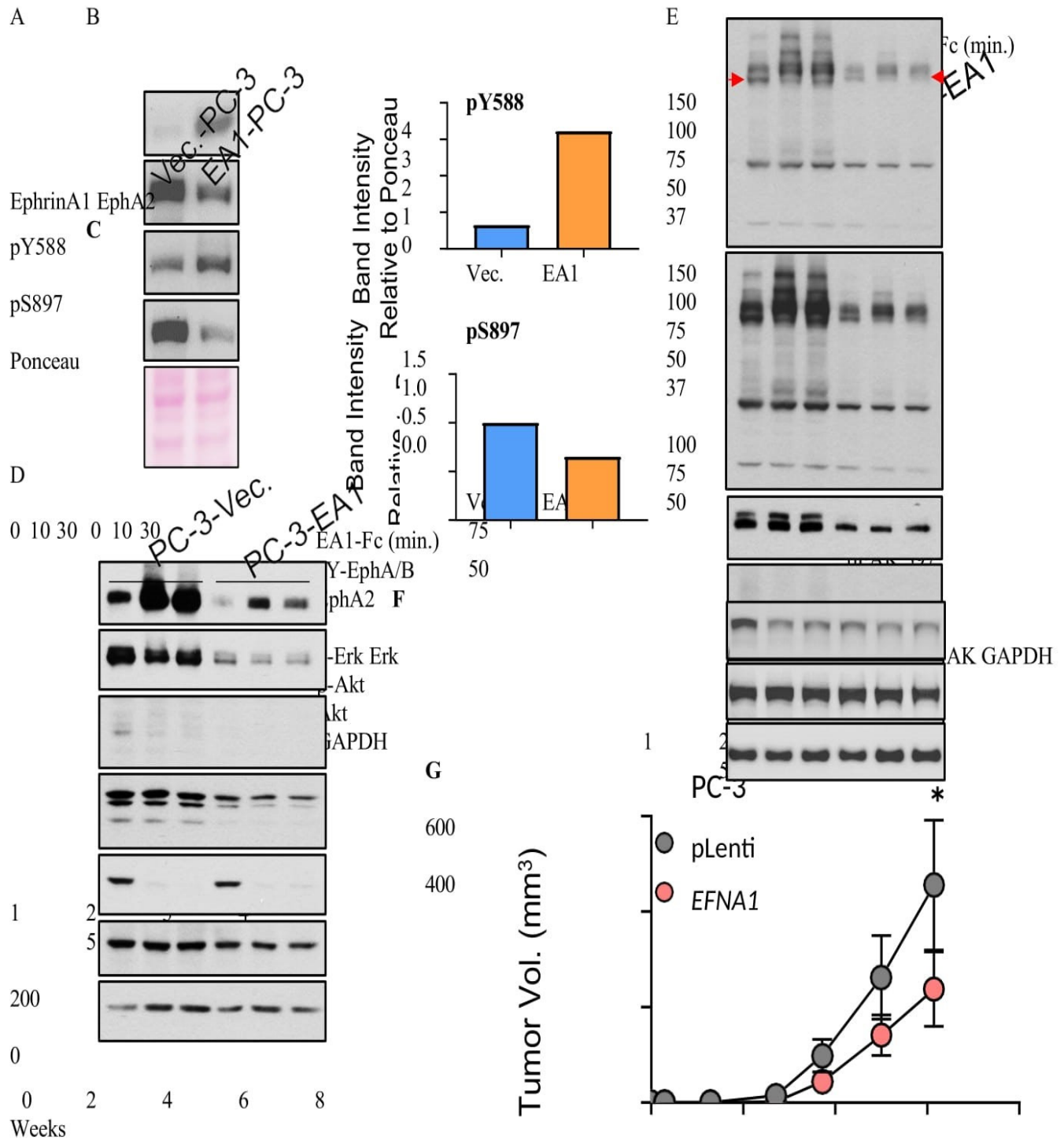


Figure 7. Restoration of EFNA1 expression in PC-3 cells suppressed oncogenic noncanonical signaling by EphA2 and inhibited subcutaneous and skeletal tumor development. **A)** Lysates of PC-3 cells transduced by lentiviral vector expressing EFNA1 (EA1) or empty control vector were subject to immunoblot with the indicated antibodies. **B,C)** Quantification of pY588 marking canonical signaling and pS897 marking non-canonical signaling by EphA2, relative to total EphA2 expression. **D)** Vec. and EA1-expressing PC-3 cells were stimulated with recombinant exogenous EA1-Fc ligand in vitro for the indicated times, and lysates were subject to immunoblot with the indicated antibodies. **E)** PY99, a monoclonal antibody that recognizes most pY motifs, was used to probe overall pY profiles using lysates from Vec. and EA1- expressing PC-3 cells stimulated with EA1-Fc. N-cadherin and pY416-Src were also probed. **F)** Analysis of cells from (E) for active FAK marked by pY397. **G)** Vec. control and EA1-expressing cells were implanted subcutaneously into nude mice. Paired t-test to be used to monitor ($p = 0.0319$). **H)** Bioluminescence imaging of mice four and six weeks after intratibial injection of PC3-vec. or PC3-EA1 expressing cells tagged with luciferase. **I)** X-ray imaging of mice 6 weeks post intratibial injection of PC3-Vec and PC3-EA1 cells.

involving many proteins across a large molecule weight range (Figure 7E, lanes 1 vs. 4, long exposure), demonstrating the powerful roles of ephrin-A1-induced activation of EphA2 in prostate cancer cell regulation. While the identities and functions for many of these tyrosine-phosphorylated proteins remained to be characterized, Src was among the molecules affected, exhibiting a robust reduction in pY416-Src (Figure 7E, lanes 1 vs. 4), the active form of the kinase. Focal adhesion kinase (FAK) is a target of Src. Consistent with our previous report [15], FAK was inactivated when upon ligand stimulation of control PC-3 cells marked by reduced pY397 (Figure 7F, lanes 1-3), and restoration of *EfnA1* led to reduced basal pY397 (Figure 7F, lanes 1 vs. 4).

Stimulation with exogenous recombinant ephrin-A1-Fc led to massive upregulation of pY in vector control cells (Figure 7D). Interestingly, ligand treatment also caused tyrosine de-phosphorylation of some proteins (Figure 7E, red arrow), including transient dephosphorylation of Src (Figure 7E, lane 1 vs. 2). The results indicate dynamic nature of EphA2 canonical signaling in controlling pY.

Expression of N-cadherin, a marker of epithelial-mesenchymal transition or EMT, was reduced in ephrin-A1-restored PC-3 cells, suggesting reversion to a less malignant phenotype. To test the effects in vivo, we implanted the vector and *EFNA1*-expressing PC-3 cells subcutaneously into immune-deficient nude mice. We found that ephrin-A1-PC-3 cells exhibited significantly diminished tumor growth relative to the vector control (Figure 7G). In aggregate, these data demonstrate the critical importance of ephrin-A1 expression and the loss of it during tumor progression in promoting malignant behaviors of prostate cancer cells.

Next, we examined how EphA2 noncanonical signaling might impact tumor development in the bone. EphA2 is preferentially overexpressed in the late-stage double-negative PCa (DNPC, Figure 1E), and is inversely correlated with AR expression. PC-3 cells have recently emerged as a model for DNPC [6,31,32,41], due to the lack of AR and neuroendocrine marker expression, while the overexpression of EphA2 and lack of ephrin-As make it a good system to examine the role of noncanonical signaling. In contrast, AR-positive cell lines generally have high ephrin-A and low EphA2 expression, rendering them unsuitable for studying noncanonical signaling by EphA2. Therefore, we utilized control and ephrin-A1-restored PC-3 cells tagged with luciferase and injected them into the tibia of nude mice. As shown in Figure 7H, mice receiving control PC-3 cells showed stronger bioluminescent imaging (BLI) signals that increased over time compared with those injected with EA1-PC-3 cells (Figure 7H). By sixth week, four of five control mice had BLI-positive tumor growth. In contrast, only one mouse injected with ephrin-A1-restored cells was positive; one lesion detectable at week four (#8) disappeared by week 6 (Figure 7H). X-ray imaging of the tibia showed evidence of bone loss characteristic of this model (red arrows) in three mice in the control group [41], only one EA1-expressing mouse displayed bone loss (Figure 7I). The intratibial injection was an imperfect model for bone metastases, as it did not happen spontaneously. However, the data did point to the importance of ligand loss on cancer cells in bone colonization.

In sum, the comprehensive characterization of EphA2-ephrin-A system in PCa using in vitro, in vivo model systems, as well

as human patient specimens from two independent Rapid Autopsy Programs demonstrates important roles of EphA2 noncanonical signaling in promoting PCa development and bone metastasis. The results also highlight overexpressed and ligand-free EphA2 in mCRPC offers attractive opportunities for development of novel therapeutic strategies targeting the receptor.

Discussion

EphA2 has come under intense investigation due to its overexpression at the late stages of many human solid tumors, including prostate cancer. However, the pathological processes it regulates, and the underlying molecular and cellular mechanisms remain incompletely understood. In this study, we show that EphA2 is selectively overexpressed in metastasis to the bone, but not visceral metastasis. Serine 897 phosphorylation that mediates the ligand-independent noncanonical signaling by EphA2 was also upregulated in bone metastasis. Loss of ephrin-A ligands on cancer cells and tumor microenvironment promotes noncanonical signaling. We find that the bone is unique among many tissues examined in expressing little of the five *EFNA* genes, providing a permissive microenvironment for the disseminating cancer cells to colonize. Consistently, analysis of human datasets shows EphA2 overexpression is associated with skeletal but not visceral metastasis, whereas loss of ephrin-A1 expression in primary PCa is correlated with poor prognosis. Further, S897A mutation that ablates EphA2 noncanonical signaling, suppressed PCa development. Restoration of ephrin-A1 expression in PC-3 cells, originally derived from bone metastasis and devoid of ephrin-As, suppressed tumor development in vivo. Together these results suggest that overexpression of EphA2 and concomitant loss of ligands in PCa lead to activation of noncanonical signaling, while the dearth of ephrin-A ligands in the bone creates a permissive microenvironment to augment skeletal metastasis.

Metastatic prostate cancer is a leading cause of cancer-related morbidity and mortality in men. Clinically, it is often manifested following androgen deprivation therapy (ADT), which leads to metastatic castration-resistant prostate cancer (mCRPC). Metastasis of prostate cancer differentially targets the bone, including vertebrae that causes pathologic fracture and spinal cord compression leading to significant neurologic and functional disability. Meta-analysis of human prostate cancer show that around 73% mCRPC patients have bone with or without LN metastases, followed by visceral disease (20.8%) and LN-only disease (6.4%) [42]. While visceral metastasis has been associated with worse overall survival, the prevalence of skeletal disease and its hitherto incurable nature make it a major health burden in men. It is widely believed that bone microenvironment lends support for mCRPC, as a result of complex interactions between the microenvironment and tumor cells. However, the exact molecular and cellular nature of such interactions remains elusive. We find that the bone is quite unique in expressing little of the five ephrin-A ligands in mammalian system, while widely expressed all other tissues examined. The lack of ephrin-As in the bone has several implications in the context of colonization and proliferation of disseminating prostate cancer cells. First, since ephrin-A ligands are anchored to the cytoplasmic membrane by GPI, EphA-ephrin-A interactions mediate cell-cell contact signaling. One of the best characterized functional outcomes of the EphA-ephrin-A

interactions is the mutual repulsion between the ligand- and receptor-presenting cells. Therefore, the dearth of ephrin-A ligand in the bone will present little resistance to the incoming prostate cancer cells overexpressing EphA2. Second, as we reported previously, ligand-induced activation of canonical signaling of EphA2 leads to strong inhibition of ERK and Akt activities, leading to reduced cell migration and proliferation [14,15].

Without the ligands to trigger tumor suppressive canonical signaling, bone microenvironment can facilitate growth and colonization of disseminated prostate cancer cells. Finally, prostate cancer progression is associated with overexpression of EphA2 and concomitant loss of ligands, conditions known to activate the ligand-independent noncanonical EphA2 signaling that enhances cancer stem cell properties and drives invasion and proliferation [12,13,43,44]. We propose that cancer cell-intrinsic changes in the balance between EphA2 and ephrin-A expression propels the selective homing and colonization of these cells in the bone. Consistent with this notion, liver expresses high levels of multiple ephrin-As and therefore represents a hostile environment for EphA2-overexpressing cells. Indeed, examination of hepatic metastases of prostate cancer collected from two Rapid Autopsy Programs showed little EphA2 expression, suggesting that the visceral disease has adopted alternatively mechanisms to take hold in the liver.

In vitro investigations reveal potential mechanisms on how the loss of ligand expression impacts the behavior of prostate cancer cells. Thus, in keeping with our previous studies [14,15], restoration of ephrin-A1 expression in metastatic PC-3 cells induced ligand-dependent canonical signaling characterized by: 1) activation of the tyrosine kinase function of EphA2 marked by pY588, concomitant with degradation of the receptor, a common mechanism of desensitization for most RTKs, 2) suppression of the oncogenic noncanonical signaling evidenced by reduced pS897, 3) inhibition of basal activation of ERK, but not Akt, and 4) reduction of N-cadherin expression, a hallmark of epithelial-mesenchymal transition. The four outputs are all in keeping with the tumor suppressor roles of EphA2 upon ligand-induced canonical signaling. Strikingly, we also observed profound changes in tyrosine phosphorylation (pY) of many proteins. While the broad trend is massive reduction of pY of many proteins, there was also notable reduction of pY in other proteins, including Src upon ligand stimulation. While the identity and function for many of these proteins in relation to EphA2 expression and signaling remain to be further investigated, the results highlight dramatic effects of ephrin-A ligand expression, or the loss of it, on global signaling and function of prostate cancer cells.

In vivo, ephrin-A1 restoration in PC-3 cells significantly impaired tumor development both subcutaneously and after implantation in the tibia. The latter was an imperfect model for bone metastases, as it did not happen spontaneously. However, the data did point to the importance of ligand loss on cancer cells in bone colonization. Supporting this notion, analysis of prostate cancer datasets from Memorial Sloan Kettering Cancer Institute showed significantly worse survival in patients who have lost ligand expression in primary prostate cancer.

Xenograft studies also demonstrated the importance of pS897 in promoting tumor development by the overexpressed EphA2, as S897A mutation that blocks S897 phosphorylation reduced growth of both PC-3 and C4-2 xenografts. Staining of metastasis tissue array prepared from patient specimens of the Rapid-Autopsy Program showed strong pS897 signals. Together these results indicate the pathological significance of the noncanonical signaling of EphA2 via pS897 in driving metastatic progression of prostate cancer.

Our findings highlight the translational significance of EphA2 in skeletal metastases of prostate cancer. As a type I transmembrane protein overexpressed on cell surface, EphA2 is amenable to a variety of targeting strategies. One strategy is the development of small molecules or monoclonal antibodies that induced the catalytic activation of EphA2, which is expected to restore its intrinsic tumor suppressor function. Indeed, we have previously discovered Doxazosin, an inhibitor of α_1 adrenergic receptor still used in the clinic, is a novel agonist for EphA2 that was able to suppress PC-3 xenograft metastasis after orthotopic injection [20,45]. Other approaches include induced degradation of the receptor. Future development of the novel EphA2-targeted agents could provide new drugs to tame the largely incurable skeletal disease of prostate cancer.

Acknowledgments

We thank Ji Zheng for the technical help. We thank the Athymic Mice and Imaging Center of the Case Comprehensive Cancer Center Shared Resources supported by P30CA043703 grant from NCI. This work was supported by NIH NIGMS T32 GM008056 (RL), National Cancer Institute training grant T32CA059366 (XS), and National Institutes of Health grants R01NS096956, R01CA250067, and R01CA155676 (BW). This work was supported by the NIH Pacific Northwest Prostate Cancer SPORE (P50CA97186) and the Institute for Prostate Cancer Research (IPCR). We thank the patients and their families, Celestia Higano, Pete Nelson, Bruce Montgomery, Elahe Mostaghel, Lawrence True, Funda Vakar-Lopez, Xiaotun Zhang, Martine Roudier, Paul Lange, Robert Vessella, and the rapid autopsy teams for their contributions to the University of Washington Medical Center Prostate Cancer Donor Rapid Autopsy Program. This work was also supported by NIH Prostate Cancer SPORE grant P50CA69568 to University of Michigan-Ann Arbor. We gratefully acknowledge the patients and families who contributed to this study through the Michigan Legacy Tissue Program.

References

1. The American Cancer Society Medical and Editorial Content Team. Key Statistics for Prostate Cancer. American Cancer Society. 2023 Apr.
2. Attard G, Parker C, Eeles RA. Prostate Cancer. *Lancet*. 2016;387:70-82.
3. Hughes R, Simons B, Hurley P. A Murine Orthotopic Allograft to Model Prostate Cancer Growth and Metastasis. *BIO-PROTOCOL*. 2017.
4. Seruga B, Ocana A, Tannock IF. Drug resistance in metastatic castration-resistant prostate cancer. *Nat Rev Clin Oncol*. 2011;8(1):12-23.

5. Park JW, Lee JK, Sheu KM. Reprogramming normal human epithelial tissues to a common, lethal neuroendocrine cancer lineage. *Science* (80-). 2018;362(6410):91-95.
6. Labrecque MP, Coleman IM, Brown LG. Molecular profiling stratifies diverse phenotypes of treatment-refractory metastatic castration-resistant prostate cancer. *J Clin Invest*. 2019.
7. Bluemn EG, Coleman IM, Lucas JM. Androgen Receptor Pathway-Independent Prostate Cancer Is Sustained through FGF Signaling. *Cancer Cell*. 2017;32(4):474-489.e6.
8. Tang F, Xu D, Wang S. Chromatin profiles classify castration-resistant prostate cancers suggesting therapeutic targets. *Science* (80-). 2024;376(6596):eabe1505.
9. Arriaga JM, Panja S, Alshalalfa M. A MYC and RAS co-activation signature in localized prostate cancer drives bone metastasis and castration resistance. *Nat Cancer*. 2020;1(11):1082- 1096.
10. Karetka MS, Sage J. Cancer origins—genetics rules the day. *Science* (80-). 2018.
11. Dhanasekaran SM, Barrette TR, Ghosh D. Delineation of prognostic biomarkers in prostate cancer. *Nature*. 2001;412(6849):822-826.
12. Pasquale EB. Eph receptors and ephrins in cancer: Bidirectional signalling and beyond. *Nat Rev Cancer*. 2010;10(3):165-180.
13. Miao H, Li DQ, Mukherjee A. EphA2 Mediates Ligand-Dependent Inhibition and Ligand- Independent Promotion of Cell Migration and Invasion via a Reciprocal Regulatory Loop with Akt. *Cancer Cell*. 2009;16(1):9-20.
14. Miao H, Wei BR, Peehl DM. Activation of EphA receptor tyrosine kinase inhibits the Ras/MAPK pathway. *Nat Cell Biol*. 2001;3(5):527-530.
15. Miao H, Burnett E, Kinch M, Simon E, Wang B. Activation of EphA2 kinase suppresses integrin function and causes focal-adhesion-kinase dephosphorylation. *Nat Cell Biol*. 2000;2(2):62-69.
16. Guo H, Miao H, Gerber L. Disruption of EphA2 receptor tyrosine kinase leads to increased susceptibility to carcinogenesis in mouse skin. *Cancer Res*. 2006;66(14):7050-7058.
17. Kania A, Klein R. Mechanisms of ephrin-Eph signalling in development, physiology and disease. *Nat Rev Mol Cell Biol*. 2016;17(4):240-256.
18. Chen P, Huang Y, Zhang B, Wang Q, Bai P. EphA2 enhances the proliferation and invasion ability of LNCaP prostate cancer cells. *Oncol Lett*. 2014;8(1):41-46.
19. Shi X, Lingerak R, Herting CJ. Time-resolved live-cell spectroscopy reveals EphA2 multimeric assembly. *Science* (80-). 2023;1050(December):1042-1050.
20. Petty A, Myshkin E, Qin H. A Small Molecule Agonist of EphA2 Receptor Tyrosine Kinase Inhibits Tumor Cell Migration In Vitro and Prostate Cancer Metastasis In Vivo. *PLoS One*. 2012;7(8):e42120.
21. Taddei ML, Parri M, Angelucci A. Kinase-Dependent and -Independent Roles of EphA2 in the Regulation of Prostate Cancer Invasion and Metastasis. *Am J Pathol*. 2009;174(4):1492- 1503.
22. Taddei ML, Parri M, Angelucci A, Bianchini F, Marconi C. EphA2 Induces Metastatic Growth Regulating Amoeboid Motility and Clonogenic Potential in Prostate Carcinoma Cells. *Mol Cancer Res*. 2011;9(2):149-160.
23. Sachdeva A, Hart CA, Kim K. Non-canonical EphA2 activation underpins PTEN-mediated metastatic migration and poor clinical outcome in prostate cancer. *Br J Cancer*. 2022;127(7):1254-1262.
24. Offenhäuser C, Dave KA, Beckett KJ. EphA2 regulates vascular permeability and prostate cancer metastasis via modulation of cell junction protein phosphorylation. *Oncogene*. 2024;(October).
25. Morrissey C, True LD, Roudier MP. Differential expression of angiogenesis associated genes in prostate cancer bone, liver and lymph node metastases. *Clin Exp Metastasis*. 2008;25(4):377-388.
26. Cerami E, Gao J, Dogrusoz U. The cBio Cancer Genomics Portal: An open platform for exploring multidimensional cancer genomics data. *Cancer Discov*. 2012;2(5):401-404.
27. Gao J, Aksoy BA, Dogrusoz U. Integrative analysis of complex cancer genomics and clinical profiles using the cBioPortal. *Sci Signal*. 2013;6(269):1-20.
28. Uhlén M, Fagerberg L, Hallström BM. Tissue-based map of the human proteome. *Science* (80-). 2015;347(6220).
29. Smith R, Liu M, Liby T. Enzalutamide response in a panel of prostate cancer cell lines reveals a role for glucocorticoid receptor in enzalutamide resistant disease. *Sci Rep*. 2020;10(1):1-13.
30. Dhanasekaran SM, Barrette TR, Ghosh D. Delineation of prognostic biomarkers in prostate cancer. *Nature*. 2001;412(6849):822-826.
31. Kaighn ME, Narayan KS, Ohnuki Y, Lechner JF, Jones LW. Establishment and characterization of a human prostatic carcinoma cell line (PC-3). *Invest Urol*. 1979;17(1):16-23.
32. Su W, Han HH, Wang Y. The Polycomb Repressor Complex 1 Drives Double-Negative Prostate Cancer Metastasis by Coordinating Stemness and Immune Suppression. *Cancer Cell*. 2019.
33. Mehra R, Tomlins SA, Yu J. Characterization of TMPRSS2-ETS Gene Aberrations in Androgen-Independent Metastatic Prostate Cancer. *Cancer Res*. 2008;68(10):3584-3590.
34. Gingrich JR, Barrios RJ, Morton RA. Metastatic prostate cancer in a transgenic mouse. *Cancer Res*. 1996;56(18):4096-4102.
35. Foster BA, Gingrich JR, Kwon ED. Advances in Brief Characterization of Prostatic Epithelial Cell Lines Derived from Transgenic Adenocarcinoma of the Mouse Prostate (TRAMP) Model1. *Cancer Res*. 1997;57:3325-3330.
36. Chen Z, Trotman LC, Shaffer D. Crucial role of p53-dependent cellular senescence in suppression of Pten-deficient tumorigenesis. *Nature*. 2005;436(August):725-730.
37. Watson PA, Ellwood-yen K, King JC, Wongvipat J, Lebeau MM, Sawyers CL, et al. Context- Dependent Hormone-Refractory Progression Revealed through Characterization of a Novel Murine Prostate Cancer Cell Line. *Cancer Res*. 2005;(24):11565-11571.
38. La Manna F, Karkampouna S, Zoni E. Metastases in prostate cancer. *Cold Spring Harb Perspect Med*. 2019;9(3):1-15.

39. Gandaglia G, Abdollah F, Schiffmann J. Distribution of metastatic sites in patients with prostate cancer: A population-based analysis. *Prostate*. 2013;74(2):210-216.
40. Kakhki VRD, Anvari K, Sadeghi R, Mahmoudian AS, Torabian-Kakhki M. Pattern and distribution of bone metastases in common malignant tumors. *Nucl Med Rev*. 2013;16(2):66-69.
41. Beltran H, Tomlins S, Aparicio A. Aggressive variants of castration-resistant prostate cancer. *Clin Cancer Res*. 2014;20(11):2846-2850.
42. Halabi S, Kelly WK, Ma H. Meta-analysis evaluating the impact of site of metastasis on overall survival in men with castration-resistant prostate cancer. *J Clin Oncol*. 2016;34(14):1652-1659.
43. Miao H, Wang B. EphA receptor signaling-Complexity and emerging themes. *Semin Cell Dev Biol*. 2011;23(1):16-25.
44. Pasquale EB. Eph receptors and ephrins in cancer progression. *Nat Rev Cancer*. 2024;24(1):5-27.
45. Petty A, Idippily N, Bobba V. Design and synthesis of small molecule agonists of EphA2 receptor. *Eur J Med Chem*. 2018;143:1261-1276.

To cite this article: Lingerak R, Petty A, Guo H, Shi X, Kim S, Lin H, et al. Bone Tropism of Prostate Cancer Metastasis is Augmented by Activation of epha2 Noncanonical Signaling and Ligand-Deficient Skeletal Microenvironment. *British Journal of Cancer Research*. 2025; 8(1): 756- 774. doi: 10.31488/bjcr.203.

© The Author(s) 2025. This is an open access article distributed under the terms of the Creative Commons Attribution License (<https://creativecommons.org/licenses/by/4.0/>).